Eur. Phys. J. A **1**, 347–354 (1998)

THE EUROPEAN PHYSICAL JOURNAL A

Study of nucleon spin-dependent properties in the resonance region*

Yu-bing Dong[1,2]

[1] CCAST(World Laboratory), P. O. Box 8730, Beijing 100080, P.R. China
[2] Institute of High Energy Physics, The Chinese Academy of Sciences, P. O. Box 918, Beijing, 100039, P.R. China[a] (e-mail: dongyb@bepc3.ihep.ac.cn)

Received: 7 October 1997
Communicated by W. Weise

Abstract. In this paper, the spin-dependent structure functions of nucleon g_1, and photoabsorption cross sections $\sigma_{1/2}$, $\sigma_{3/2}$ and σ_T in the resonance region are estimated based on the constituent quark model and the properties of the five phenomenological Breit-Wigner resonances $P_{33}(1232)$, $S_{11}(1535)$, $D_{13}(1520)$, $P_{11}(1440)$, and $F_{15}(1680)$. Our results are compared to the recent E143 data of the polarized structure functions $g_1(W^2, Q^2)$ at points $Q^2 = 0.5GeV^2$ and $Q^2 = 1.2GeV^2$ and the data of the total inclusive photoabsorption cross sections.

PACS. 14.20.Dh Protons and neutrons – 13.60.Hb Total and inclusive cross sections (including deep inelastic processes) – 12.39.Ki Relativistic quark model – 25.45.De Elastic and inelastic scattering

1 Introduction

Investigations of the spin physics both in the deep-inelastic scattering and resonance regions are very important issues both in theoretical and experimental physics. Nowadays, considerable attention has been paid to the nucleon spin-dependent properties, such as the polarized structure functions $g_1(x, Q^2)$ [1-3], in the resonance region. This is because at the limit $Q^2 \to 0$, the negative value of the Gerasimov-Drell-Hearn (GDH) sum rule [4] constrains the integral of the polarized structure functions $g_1(x, Q^2)$ [5] to be

$$I_1(Q^2) = \int_0^1 g_1(x, Q^2)dx = -\frac{\nu_{th}}{4M}\kappa^2. \qquad (1)$$

In (1) ν_{th} is the threshold energy of pion photoproduction

$$\nu_{th} = \frac{Q^2 + 2m_\pi M + m_\pi^2}{2M}, \qquad (2)$$

and M, m_π, and κ are nucleon, π-meson masses, and nucleon anomalous magnetic moment, respectively. It has been demonstrated [6] that the GDH sum rule and the integral of the polarized structure function $I_1(Q^2)$ in the resonance region are very important for us to understand the data of European Muon Collaboration (EMC) [7] in the deep inelastic scattering region (DIS). Moreover, we know that in the resonance region, low-lying resonances, such as the $P_{33}(1232)$, play a dominant role to explain the polarized structure function and the GDH sum rule [8-9]. Therefore, the investigation of the Q^2-dependent behavior of $I_1(Q^2)$ would shed light on baryon resonance properties. In addition, we also know the duality that the integral of the polarized structure function $I_1(Q^2)$ could be explained by either deep-inelastic and resonance languages, as a result, the study of $I_1(Q^2)$ in the resonance region would allow us to extract matrix elements of higher-twist operators from the data [10].

Recently, E143 collaboration [11] in SLAC has reported their first measurement for the proton and deuteron structure functions in the region of the nucleon resonance for $W^2 < 5GeV^2$ (W is center of mass energy) at two fixed momentum transfer points: $Q^2 \sim 0.5GeV^2$ and $Q^2 \sim 1.2GeV^2$. This is the first information on the Low-Q^2 evolution of the integral $I_1(Q^2) = \int_0^1 g_1(x, Q^2)dx$ (They expressed the integral as $\Gamma(Q^2)$) toward the GDH limit at $Q^2 = 0$. In their work, the contribution from the baryon resonances $\Gamma_{res}(Q^2)$ is modeled by dividing the resonance region into three parts [11,12] and adjusting the asymmetries for the dominant resonances, such as the $P_{33}(1232)$, $S_{11}(1535)$, $D_{13}(1520)$, and $F_{15}(1680)$, in each resonance part using the three independent parameters. It is believed that these new data are very crucial to understand the polarized structure functions in the resonance region and are also important to test different model calculations. The forthcoming experiments at MAMI [13] in Mainz, SPring-8 [14], and Jefferson Lab [15] are expected to give out more accurate data both for the direct checking the GDH sum

* Supported by National Natural Science Foundation of China(NSFC)
[a] Mailing address

rule and the Q^2-dependent behavior of the integral $I_1(Q^2)$ of the polarized structure functions in the resonance region.

On the other hand, we know that the polarized structure function also closely connects the other nucleon spin-dependent properties, such as the photoabsorption cross sections. This feature can be seen clearly from the definition of $g_1(x,Q^2)$ [16]

$$g_1(x,Q^2) = \frac{MK}{8\pi^2\alpha(1+\frac{Q^2}{\nu^2})} \times [\sigma_{1/2}(\nu,Q^2) - \sigma_{3/2}(\nu,Q^2) + \frac{2\sqrt{Q^2}}{\nu}\sigma_{TS}(\nu,Q^2)], \quad (3)$$

where K is photon flux, $\sigma_{1/2}(\nu,Q^2)$ and $\sigma_{3/2}(\nu,Q^2)$ are two spin-dependent transverse photoabsorption cross sections for the polarized nucleon with its helicity antiparllel and parallel to the helicity of the polarized photons, respectively. $\sigma_{TS}(\nu,Q^2)$ represents the interference between the transverse and longitudinal currents. The GDH sum rule which reads

$$-\frac{\kappa^2}{4} = \frac{M^2}{8\pi^2\alpha}\int^{\infty}\frac{d\nu}{\nu}(\sigma_{1/2}(\nu) - \sigma_{3/2}(\nu)), \quad (4)$$

relates the spin-dependent photoabsorption cross sections directly. It connects the helicity structure of the cross sections in the inelastic region with ground state properties [17]. Therefore, the studies of the Q^2-dependent behavior of the integral $I_1(Q^2)$ and the GDH sum rule are very crucial for us to understand the photoabsorption cross sections. Recently, the new measurements of the photoabsorption cross sections for ^1H, ^2H, and ^3He by M. MacCormick et al.[18] and for Li, Be, C, Al, Pb, Sn, and U up to 1.2GeV by the group of Frascati and Mainz group [19-21] have been published. It is believed that the first and second resonance peaks of the total inclusive cross sections are contributed by the $P_{33}(1232)$ and $S_{11}(1535)$ and $D_{13}(1520)$ dominantly. These new data presented the total inclusive photoabsorption cross sections per nucleon in the low energy range. Comparing to the total photoabsorption cross sections on nuclei, we expect that the investigation of the total photoabsorption cross sections on nucleon could show the nucleon medium effect, such as "damping" in nuclei [22-23].

In this paper, based on the simple constituent quark model, we will use the Breit-Wigner resonances $P_{33}(1232)$, $S_{11}(1535)$, $D_{13}(1520)$, $P_{11}(1440)$, and $F_{15}(1680)$ to qualitatively describe the E143 data of the polarized structure functions and the data in [18,21] of the total inclusive photoabsorption cross sections in the resonance region. In our calculations, the simple phenomenological Breit-Wigner formula is utilized to express the one-pion, one η, and two-pion decay modes of the five dominant resonances. Furthermore, the role of the two-pion decay modes and the effect of the interference cross section σ_{TS} will also be addressed.

2 Parameterization of the elementary γN cross section

For the resonance contribution to the total inclusive photoabsorption cross sections, we use the Breit-Wigner ansatz [24] under the assumption that the complex phase of the amplitudes is equal to the phase of the resonance propagator [22-24]. If we only consider the one-pion decay channel of the resonances, the total inclusive resonance absorption cross section is

$$\sigma_T = \sigma_{\gamma N\to R\to N\pi} = \frac{1}{2}(\sigma_{1/2}+\sigma_{3/2}) = (\frac{k_R}{k})^2\frac{W^2\Gamma_\gamma\Gamma_{R\to N\pi}}{(W^2-M_R^2)^2+W^2\Gamma_{total}^2}\frac{2M}{M_R\Gamma_R} \times(\mid A_{1/2}\mid^2 + \mid A_{3/2}\mid^2), \quad (5)$$

where

$$\Gamma_\gamma = \Gamma_R(\frac{k}{k_R})^{j_1}(\frac{k_R^2+X^2}{k^2+X^2})^{j_2}, \quad X = 0.3GeV. \quad (6)$$

In above two equations, j_1, j_2, and Γ_R are the resonance's parameters. They are quoted from [22-25] and Particle Data Group [26]. The parametrized one-pion decay width is

$$\Gamma_{R\to N\pi}(q) = \Gamma_R\frac{M_R}{M}(\frac{q}{q_R})^3(\frac{q_R^2+c^2}{q^2+c^2})^2, \quad c = 0.3GeV, \quad (7)$$

for the $P_{33}(1232)$, and

$$\Gamma_{R\to N\pi}(q) = \Gamma_R(\frac{q}{q_R})^{2l+1}(\frac{q_R^2+\delta^2}{q^2+\delta^2})^{l+1} \quad (8)$$

for the $D_{13}(1520)$, $P_{11}(1440)$, and $F_{15}(1680)$. In (5), l is the angular momentum of the emitted meson and $\delta^2 = (M_r - M - m_\pi)^2 + \frac{\Gamma_R^2}{4}$. In (5)-(8) k and q are the photon and pion 3-momentum in the cms for a given center of mass energy W, k_R, q_R, and Γ_R are taken at the pole of the resonance. For the resonance $S_{11}(1535)$, the ηN decay mode is also considered in this paper. The decay widths of the πN and ηN processes of the $S_{11}(1535)$ are [27]

$$\Gamma_{R\to\pi(\eta)} = \frac{q_{\pi(\eta)}}{q}b_{\pi(\eta)}\Gamma_R\frac{q_{\pi(\eta)}^2+c_{\pi(\eta)}^2}{q^2+c_{\pi(\eta)}^2}, \quad c_{\pi(\eta)}^2 = 0.25GeV^2, \quad (9)$$

where $b_{\pi(\eta)}$ is the $\pi(\eta)$ branching ratio. These phenomenological expressions for the one-pion and one η decay widths implies the constraint condition $W \geq M + m$ (m is emitted meson mass), namely, the consideration of the meson photoproduction threshold behavior.

In this paper, besides the contribution of the decay channel πN of the five important resonances $P_{33}(1232)$, $S_{11}(1535)$, $D_{13}(1520)$, $P_{11}(1440)$, and $F_{15}(1680)$ and the decay channel ηN of the $S_{11}(1535)$, the two-pion decay mode of the $S_{11}(1535)$, $D_{13}(1520)$, $P_{11}(1440)$, and

$F_{15}(1680)$ is also considered phenomenologically. According to [22-23,25], this process is assumed that a high lying baryon resonance R decays first into a $P_{33}(1232)$ or $P_{11}(1440)$ and a pion or into a nucleon and $\rho-$ or σ meson. Then, the new resonance R eventually decays into a nucleon and pion or a nucleon and two pions. It is parametrized as a two-step process:

$$R \to ra \to N\pi\pi,$$

where r stands for a baryonic or mesonic resonance, such as the $P_{33}(1232)$, $P_{11}(1440)$, ρ or σ and a is a pion or nucleon. The phenomenological description of the two-pion decay width has been studied in [22,23,25]. In this paper, we follow their investigations to write the width as a phase space weight integral over the mass distribution of the intermediate resonance:

$$\begin{aligned}&\Gamma_{R\to ra}(W) \\ &= \frac{k'}{W}\int_0^{W-m_a} d\mu p_f \frac{2}{\pi}\frac{\mu^2\Gamma_{r,tot}(\mu)}{(\mu^2-m_r^2)^2+\mu^2\Gamma_{r,tot}^2(\mu)} \\ &\times\frac{(M_R-M-2m_\pi)^2+c^2}{(W-M-2m_\pi)^2+c^2}, \quad with \quad c=0.3GeV,\end{aligned} \tag{10}$$

where, k' is a parameter which is defined by a constraint condition that when $W = W_R$, $\Gamma_{R\to ra}(W_R)$ fits the experimental data, p_f is the momentum of r and a in the restframe of the high-lying resonance R. $\Gamma_{r,tot}$ is the total width of the resonance r. The decay width of meson resonances is parametrized similarly to that of the $P_{33}(1232)$

$$\Gamma(\mu) = \Gamma_r \frac{M_r}{\mu}(\frac{q}{q_r})^{2J_r+1}\frac{q_r^2+\delta^2}{q^2+\delta^2}, \quad \delta = 0.3GeV, \tag{11}$$

where m_r and μ are the mean mass and actual mass of the meson resonance, q and q_r are the pion three-momenta in the restframe of the resonance with masses M_r and μ, J_r and Γ_r are the spin and decay width of the resonance at the resonance pole, respectively.

In our calculation, the resonance transverse helicity amplitudes $A_{1/2}$ and $A_{3/2}$ in (5) are calculated by using the simple constituent quark model as usual [28-29],

$$\begin{aligned}A_{1/2} &= < R, J_z = 1/2 \mid H_T \mid N, J_z = -1/2 >, \\ A_{3/2} &= < R, J_z = 3/2 \mid H_T \mid N, J_z = 1/2 >,\end{aligned} \tag{12}$$

where N and R stand for nucleon and baryon resonance, H_T is transverse photon-quark interaction Hamiltonian. In nonrelativistic approximation, the impulse photo-quark interaction reads [28]

$$\begin{aligned}H_T = \sum_j [&e_j \boldsymbol{r}_j \cdot \boldsymbol{E}_j - \frac{e_j}{2m_j}\boldsymbol{\sigma}_j \cdot \boldsymbol{B}_j - \frac{e_j}{4m_j}\boldsymbol{\sigma}_j \\ &\cdot(\boldsymbol{E}_j \times \frac{\boldsymbol{p}_j}{2m_j} - \frac{\boldsymbol{p}_j}{2m_j}\times \boldsymbol{E}_j)] \\ &+ \sum_{j<l}\frac{1}{4M_T}[\frac{\boldsymbol{\sigma}_j}{m_j} - \frac{\boldsymbol{\sigma}_l}{m_l}]\cdot(e_l\boldsymbol{E}_l \times \boldsymbol{p}_j - e_j \boldsymbol{E}_j \times \boldsymbol{p}_l),\end{aligned} \tag{13}$$

where the electric and magnetic fields are defined as

$$\begin{aligned}\boldsymbol{E}_i &= i\nu\sqrt{4\pi}\sqrt{\frac{1}{2\nu}}\boldsymbol{\epsilon} exp(-\boldsymbol{k}\cdot\boldsymbol{r}_i), \\ \boldsymbol{B}_i &= i\sqrt{4\pi}\sqrt{\frac{1}{2\nu}}\boldsymbol{\epsilon}\times\boldsymbol{k} exp(-i\boldsymbol{k}\cdot\boldsymbol{r}_i).\end{aligned} \tag{14}$$

To calculate the longitudinal transition amplitude $S_{1/2} = < R, J_z = 1/2 \mid J_0 \mid N, J_z = 1/2 >$ for the interference cross section term σ_{TS} in (3), we employ the longitudinal transition operator[30]

$$\begin{aligned}J_0 = \sqrt{\frac{1}{2\omega}}\{&\sum_j (e_j + \frac{ie_j}{4m_j^2}\boldsymbol{k}\cdot(\boldsymbol{\sigma}_j\times\boldsymbol{p}_j))e^{i\boldsymbol{k}\cdot\boldsymbol{r}_j} \\ &-\sum_{j<l}\frac{i}{4M_N}(\frac{\boldsymbol{\sigma}_j}{m_j} - \frac{\boldsymbol{\sigma}_l}{m_l}) \\ &\cdot(e_j\boldsymbol{k}\times\boldsymbol{p}_l e^{i\boldsymbol{k}\cdot\boldsymbol{r}_j} - e_l\boldsymbol{k}\times\boldsymbol{p}_j e^{i\boldsymbol{k}\times\boldsymbol{r}_l}\}.\end{aligned} \tag{15}$$

It should be emphasized that both the transition operators H_T and J_0 have the spin-orbit terms (the third and the second terms in (13) and (15)) and the non-additive terms (the last terms in (13) and (15)). These relativistic corrections have been demonstrated to be very important for the theoretical derivation of the well-known model-independent GDH and Schwinger sum rules for g_1 and g_2 in the real photon limit $Q^2 \to 0$ [9] and the low energy theorem in Compton scattering. Therefore, the relativistic corrections in the transition operators should be considered consistently. In addition, in our calculation, we regard the Roper resonance $P_{11}(1440)$ as a hybrid state and use the parameterization form of Li, Burkert, and Li [31] to describe its rapid falloff with Q^2 in accordance with the data.

To study the integral of the polarized structure function $I_1(Q^2)$ we define the variable $x = \nu_{th}/\nu$ in the resonance region. Then

$$I_1(Q^2) = \int_{\nu_{th}}^{\infty} g_1(\nu, Q^2)\frac{\nu_{th}}{\nu^2}d\nu, \tag{16}$$

where ν_{th} is defined in eq. (2). In eq.(16), the variable x is the same as the conventional Bjorken variable $x_B = \frac{Q^2}{2M\nu}$ in the deep inelastic region ($Q^2 \to \infty$). The lower limit ν_{th} in above integral is consistent with the Breit-Wigner formula in (7-8) for the one-pion decay widths of the resonances because the meson photoproduction threshold behavior is considered. It also means the integral does not include any elastic contribution [5,10,32], namely, it only includes the inelastic resonance contribution.

In Figs.1-4, the five Breit-Wigner resonance contributions to the proton and deuteron polarized structure functions $g_1(W^2, Q^2)$ at $Q^2 = 0.5GeV^2$ and $Q^2 = 1.2GeV^2$ are displayed in the range $(M+m_\pi)^2 < W^2 < 4GeV^2$ in comparison with the recent E143 [11] data. In the Figs. 2 and 4, the results for the deuteron are calculated using the following simple relation among the proton, neutron, and deuteron polarized structure functions

$$g_1^d(x, Q^2) = \frac{1-\frac{3}{2}\omega_D}{2}[g_1^p(x, Q^2) + g_1^n(x, Q^2)], \tag{17}$$

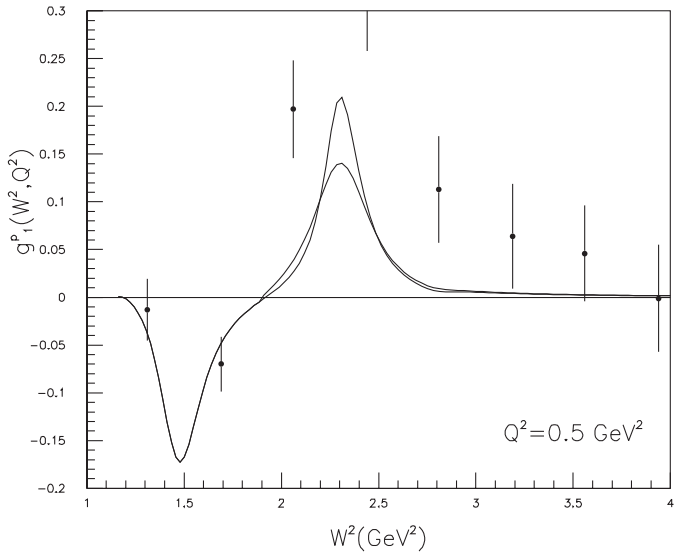

Fig. 1. $g_1(W^2, Q^2)$ as a function of W^2 for proton at $Q^2 = 0.5GeV^2$. The data are quoted from [11]. The *solid* and *dashed curves* are the results with and without consideration of the two-pion decay channel. The *full error bars* correspond to the statistical and systematic errors added in quadrature

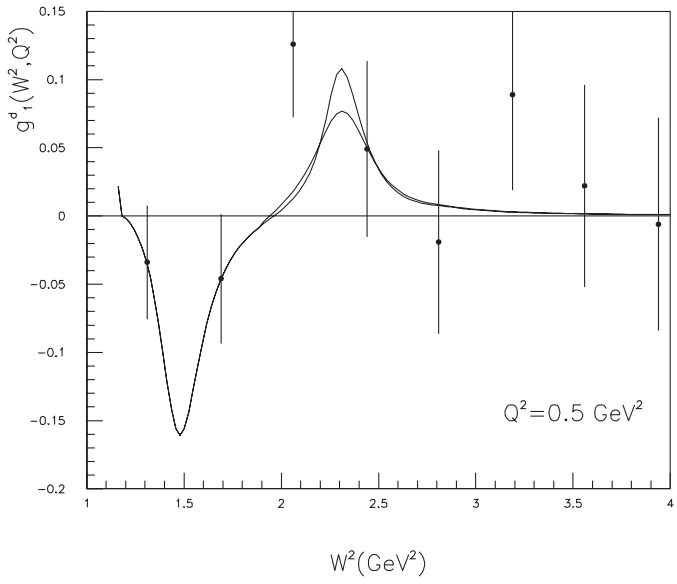

Fig. 2. Same as in Fig. 1, but for deuteron

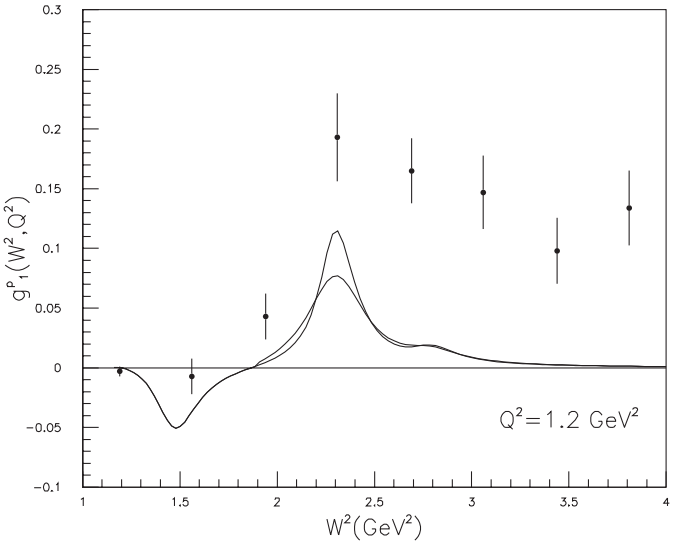

Fig. 3. Same as in Fig. 1, but at $Q^2 = 1.2GeV^2$

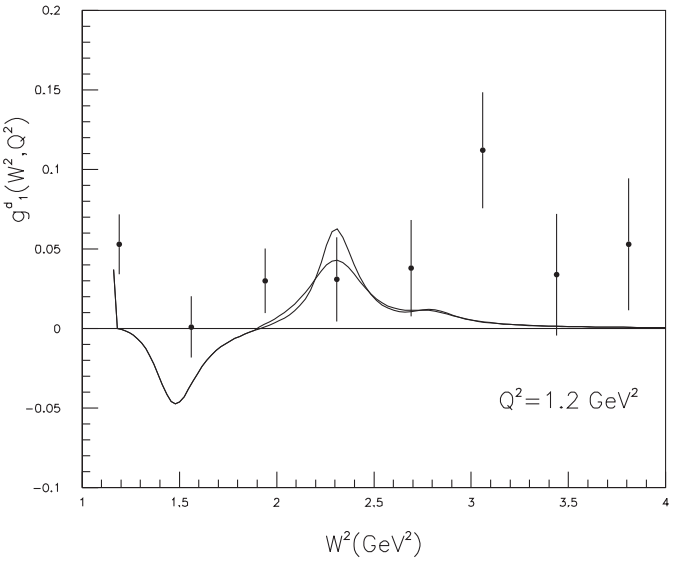

Fig. 4. Same as in Fig. 3, but for deuteron

where ω_D is D-wave admixture ($\omega_D \sim 5\%$) of the deuteron wave function. To illustrate the effect of the two-pion decay mode of the resonances $P_{11}(1440)$, $S_{11}(1535)$, $D_{13}(1520)$, and $F_{15}(1680)$ explicitly, we also, in the two figures, draw the corresponded results without the consideration of the two-pion decay channel. In Figs.5-6, we depict our total predictions for the integral of the polarized structure function $I_1(Q^2)$ for the proton and neutron targets. These total results are the combination of the resonance and nonresonant contributions [5,9]. The nonresonant part, which stands for the contribution from the unmeasured small-x region, is obtained by using the third parameterization method of E143 [33] for $Q^2 > 0.3GeV^2$ (see the work of Li and Dong in [9] for detail explanation of theoretical estimation of the nonresonant contribution). This parametrization method assumed the ratios g_1^p/F_1^p, and g_1^d/F_1^d are Q^2-dependent. In the paper of E143 group [33], they found that the assumption that g_1 and F_1 have approximately the same Q^2-dependence was consistent with all available data in the deep inelastic region $Q^2 > 1GeV^2$. However, at lower Q^2 region, there are significant deviations from this assumption. In Figs. 5-6, the recent E143 data Γ_{tot} at the points $Q^2 = 0.5GeV^2$ and $Q^2 = 1.2GeV^2$ are plotted in comparison with our results. In order to explicitly indicate the effect of the term σ_{TS} in (3), which means the interference cross section between the longitudinal and transverse currents, on the integral $I_1(Q^2)$, in Fig. 7, we display a comparison of the Breit-Wigner resonance contributions to the integral of proton

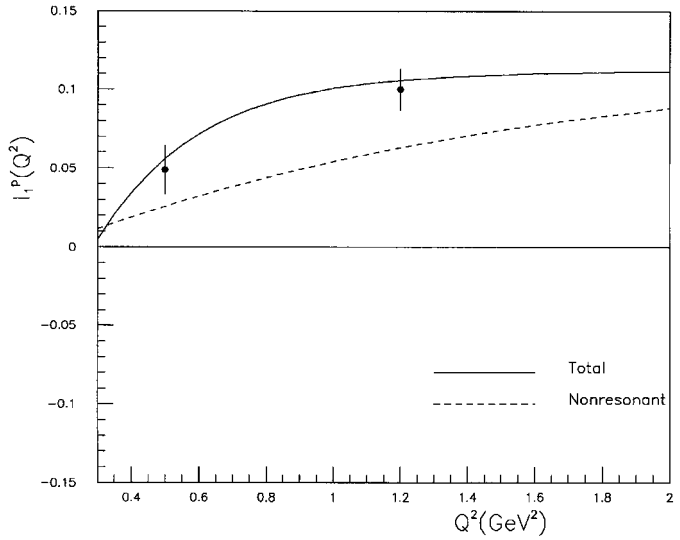

Fig. 5. Integral of the polarized structure function $I_1(Q^2)$ for proton. The *solid* and *dashed curves* are the total and nonresonant results, respectively. The data are Γ_{tot} in [11]. The *full error bars* correspond to the statistical and systematic errors added in quadrature

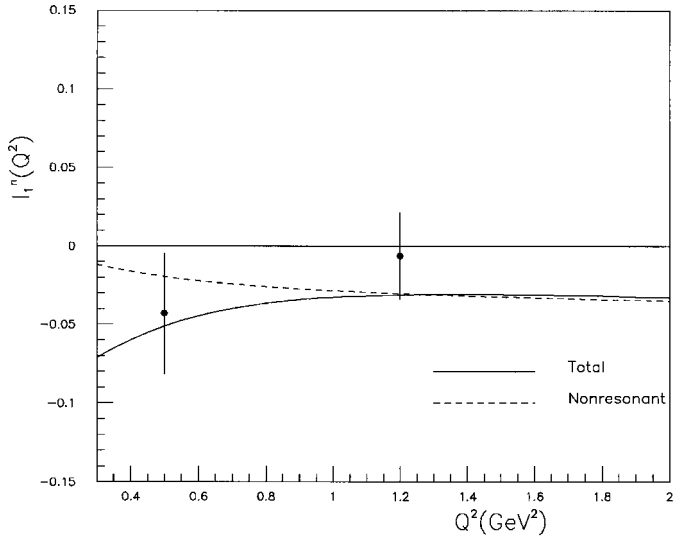

Fig. 6. Same as in Fig. 5, but for neutron

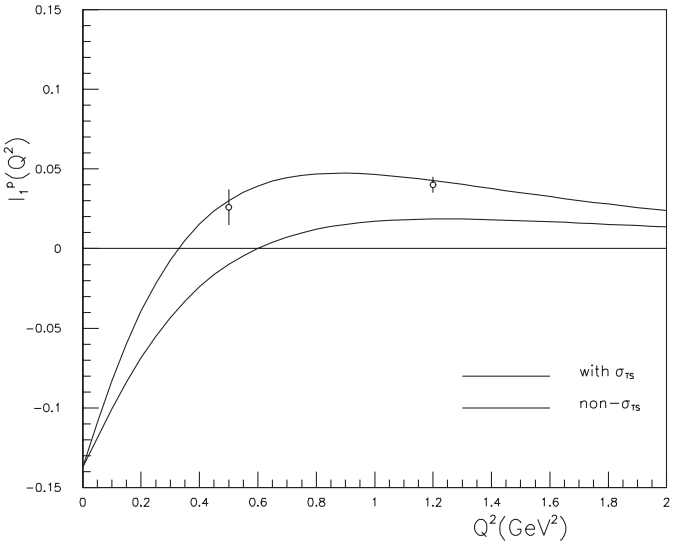

Fig. 7. Contribution from the five Breit-Wigner Resonances to the integral $I_1(Q^2)$. The *solid* and *dashed curves* are the calculations with and without the consideration of the interference term σ_{TS}. The data are Γ_{res} in [11]. The *full error bars* correspond to statistical and systematic errors added in quadrature

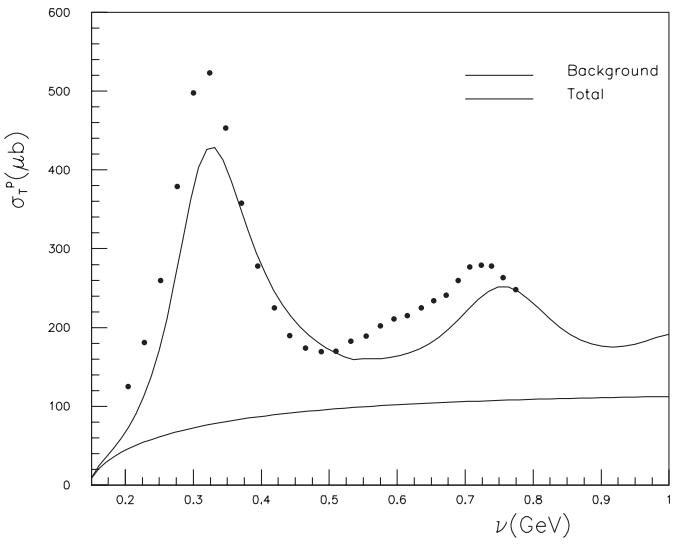

Fig. 8. Total inclusive photoabsorption cross section for proton target in the real photon limit. The *solid* and *dashed curves* are the total cross section and the background cross section, respectively. The data are quoted from [18]

with and without the term. In the figure, the data of E143 group extracted from measured resonance region Γ_{res} are also shown for proton target for the two fixed Q^2 points.

In Figs. 8-9, the total inclusive photoabsorption cross sections for the proton and neutron targets in the real photon limit are illustrated compared to the new data of [18,21], respectively. In the two figures, the background contributions are calculated based on the phenomenological parameterization forms of [34] for proton and neutron for simplicity. The total results are the sum of the resonance and background contributions incoherently. In Figs. 10-11, the resonance contributions to the photoabsorption cross sections for proton and neutron are shown for comparison. In this two figures, the contributions without the two-pion decay channel are also drawn. In Fig. 12, the spin-dependent photoabsorption cross sections $\sigma_{1/2}$ and $\sigma_{3/2}$, and the difference $\sigma_{1/2}-\sigma_{3/2}$ contributed by the five Breit-Wigner resonances in the real photon limit are plotted for proton target. We believed that this theoretical prediction for the spin-dependent photoabsorption cross sections is very important for direct checking the GDH sum rule in MAMI [13] and SPring-8 [14] in the near future.

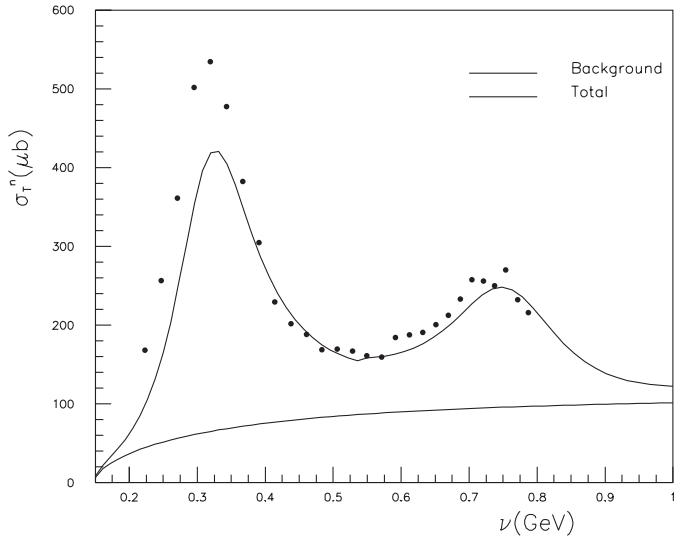

Fig. 9. Same as in Fig. 8, but for neutron. The data are quoted from [21]

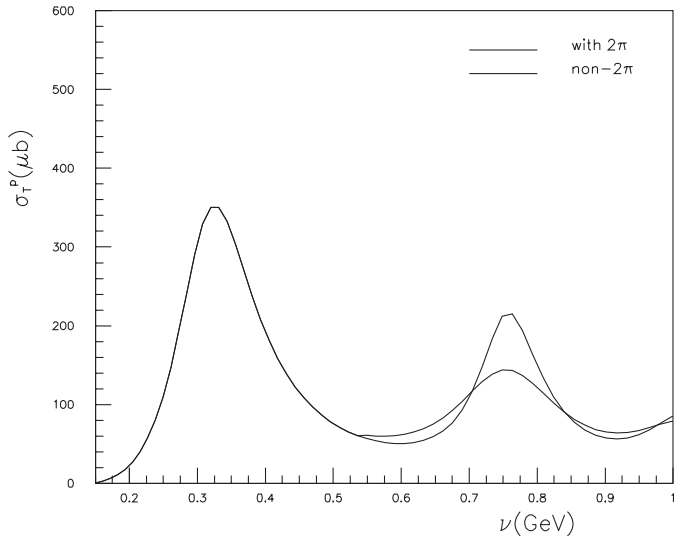

Fig. 10. Contribution from the five Breit-Wigner resonances to the total inclusive photoabsorption cross section of proton target in the real photon limit. The *solid* and *dashed curves* are the results with and without consideration of the two-pion decay mode, respectively

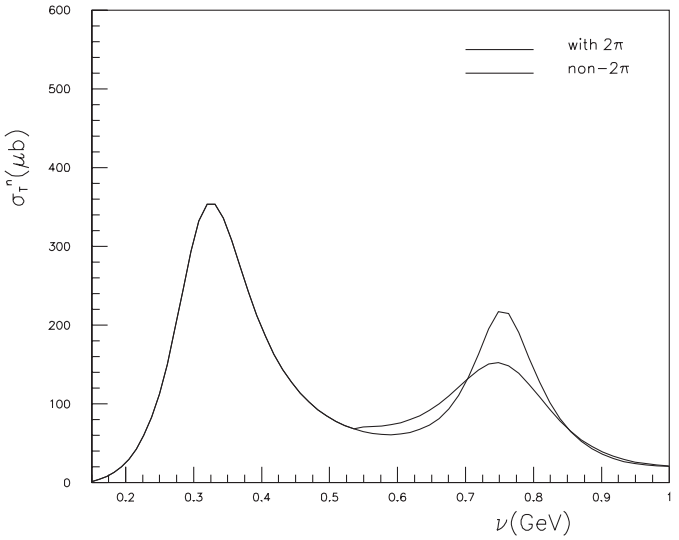

Fig. 11. Same as Fig. 10, but for neutron

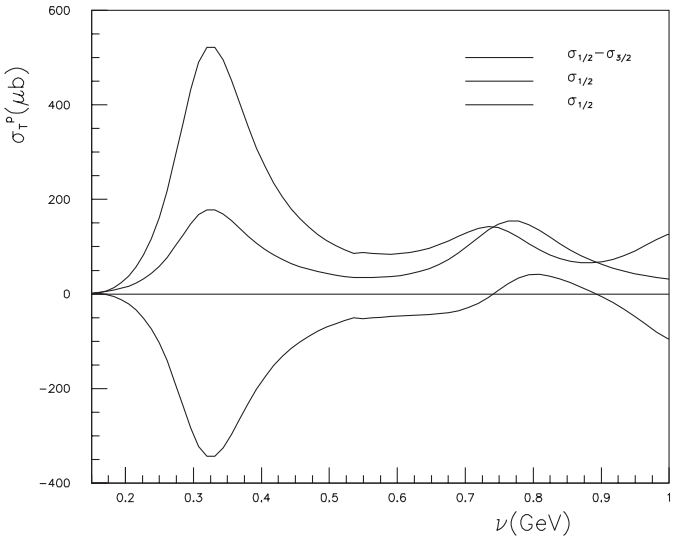

Fig. 12. Theoretical predictions for the spin-dependent photoabsorption cross sections for proton target in the real photon limit. The *solid, dashed*, and *dotted curves* stand for the resonance contributions to $\sigma_{1/2}$, $\sigma_{3/2}$, and $\sigma_{1/2}-\sigma_{3/2}$, respectively

3 Concluding remarks

From Figs. 1-4, one can see that our simple constituent quark model and the five phenomenological Breit-Wigner resonances could predict the proton and deuteron polarized structure functions $g_1(W^2, Q^2)$ qualitatively when compared with the recent E143 data. Particularly, in the small W region, the contributions of the five resonances are dominant. Our results indicate the success of the constituent quark model. In Figs. 1-4, one sees that the effects of the two-pion decay mode of the resonances $P_{11}(1440)$, $S_{11}(1535)$, $D_{13}(1520)$ $F_{15}(1680)$ are not remarkable. This is because the branching ratios of this decay channel are small. Among the four resonances, the largest branching ratio of this channel is 40% for the resonance $D_{13}(1520)$. The difference that appears in the second peak illustrates the effects of the two-pion decay channel. In fact, there are still discrepancies between the data and the present qualitative theoretical calculations. For example, the difference at large W range and the poor calculated results at $Q^2 = 1.2GeV^2$ comparing with the results at $Q^2 = 0.5GeV^2$. In our calculations, we find that the consideration of the two-pion decay channel could improve our prediction slightly for the polarized structure function $g_1(W^2, Q^2)$. The large difference of $g_1(W^2, Q^2)$ between the data and our work in the large W range might be due to the fact that we overlook the effects of the other resonances, such as $S_{31}(1620)$, $F_{37}(1950)$, $D_{33}(1700)$, $P_{13}(1720)$, and $F_{35}(1905)$. Our qual-

itative calculations indicate that our present model could roughly describe the first two peaks of the proton and deuteron polarized structure functions $g_1(W^2, Q^2)$. However, it should be improved further.

In our work, we find that the phenomenological Breit-Wigner descriptions for the one-pion, one η and two-pion decay modes are important to lower the crossing point of the integral $I_1(Q^2)$ of the proton polarized structure function. The crossing point which means that at this Q^2 point the integral of the polarized structure function equals zero. We know that the Q^2-dependent behavior of the integral has two sum rules, one is associated with the GDH sum rule in the real photon limit which constrains the integral of g_1 to be a negative value and another is the Ellis-Jaffe sum rule in the deep inelastic scattering range which makes the integral to be positive. Therefore, there is a crossing point of the Q^2-evolution of I_1. This sign change point is very important because it represents the crossover from the short-distance physics, where the perturbative QCD works, to nonperturbative physics [35]. Our calculated sign change point is $Q^2 \sim 0.33 GeV^2$. This value is much smaller than the previous results of Burkert et al. ($0.8 GeV^2$)[8] and Li and Dong ($0.55 GeV^2$) [9]. It should be stressed that the present result is much favored by the recent E143 data, because at $Q^2 = 0.5 GeV^2$, the E143 data show that the resonance contribution is positive $\Gamma_{res}(Q^2) = 0.026 \pm 0.008 \pm 0.008$ [11]. The data and our calculated result indicate that the rigorous description for the resonance properties is necessary when compared with the previous work [8,9]. Moreover, our calculation also confirms that GDH sum rule is largely saturated by the low-lying resonances. Our result for the contribution from resonances to the GDH sum rule at $Q^2 \to 0$ is

$$\Gamma(Q^2) = \frac{M\nu_{th}}{8\pi^2\alpha} \int_{\nu_{th}}^{\infty} \frac{(\sigma_{1/2} - \sigma_{3/2})}{\nu} d\nu \simeq -0.118$$

for proton target. Comparing eq.(1) with above result, one can get the corresponding anomalous magnetic moment for proton $\kappa_p \simeq 1.72$. These result is consistent with the experimental data. In addition, from Fig. 7, we see that the interference term σ_{TS} also plays a role on the integral I_1, particularly, it shows its explicit effect in the small Q^2 range. According to the analysis of Li and Dong [9], one sees that the term is essential to get the Schwinger sum rule of the polarized structure function $g_2(x, Q^2)$. Therefore, to study the Q^2-dependent behavior of the integral $I_1(Q^2)$ in the resonance region, one should take the term into account. This conclusion disagrees with the E143 analysis. In their work, they ignored the longitudinal current contribution and assumed $g_1 = -g_2$ [11].

Since at present the experimental data [18,21] are available for the total inclusive photoabsorption cross sections, it is interesting to compare our model predictions to those data [18,21]. From Figs. 8-9, one can see that our simple constituent quark model calculations are roughly consistent with the data for the total photoabsorption cross sections for the proton and neutron. It is obvious that the first peak is contributed by the first excited state $P_{33}(1232)$, the second one originates from the other two resonances $S_{11}(1535)$ and $D_{13}(1520)$, particularly, from $D_{13}(1520)$ at low Q^2. However, theoretical predictions could not fit the corresponding data well quantitatively. One reason for the discrepancies is the background treatment. In fact, our empirical consideration for the background is rather arbitrary and not enough, since we ignore any interferences between the background and resonance contributions of the same multipoles [36]. Another one is the omission of the other resonances, such as $S_{31}(1620)$, $F_{37}(1950)$, $D_{33}(1700)$, $P_{13}(1720)$, and $F_{35}(1905)$. Those are expected to play a role at larger ν range. To check the resonance contributions to the total photoabsorption cross sections in Figs. 10-11, one finds that the two-pion decay mode plays an explicit role in the second peak. It improves the theoretical prediction in the intermediate ν range between the first and the second peak. Finally, Fig. 12 shows an important theoretical prediction for the spin-dependent cross sections $\sigma_{1/2}$, $\sigma_{3/2}$ and their difference $\sigma_{1/2} - \sigma_{3/2}$. So far, there are no any data available for these values. We expect these calculated results would be tested in the forthcoming experiments on the GDH sum rule direct checking.

To summarize this paper, we have estimated the proton and deuteron polarized structure functions $g_1(W^2, Q^2)$ at $Q^2 = 0.5 GeV^2$ and $Q^2 = 1.2 GeV^2$ points based on our simple constituent quark model and the five Breit-Wigner resonances including the two-pion decay mode. Comparing with the E143 data, one can conclude that our simple calculations are roughly successful. Our predictions for the integral of the polarized structure functions $I_1(Q^2)$ and the total photoabsorption cross sections for the proton and neutron targets agree with the data qualitatively. The discrepancies in $g_1(W^2, Q^2)$ between our predictions and data imply the limitation of our present simple constituent quark model and they also mean that other new ingredients should be considered. It is believed that the dynamical model for pion photoproduction [37] might improve the theoretical predictions. Moreover, we see that the consideration of the background is rather simple and phenomenological. A more intensive and coherent investigation of the background and the resonance contributions to the photoabsorption cross sections [38] is needed.

References

1. S. D. Drell, SLAC Report No. SLAC-PUB 5720, 1992(unpublished); F. E. Close, In Hadronic Physics in the 1990's with Multi-GeV Electrons, Proceedings of the first European workshop, Seillac, France, 1988, edited by B. Frois et al.,[Nucl. Phys. A**497** (1989) 109c]; B. L. Ioffe, Surveys in High Energy Physics, **8** (1995), 107
2. M. Anselmino, B. L. Ioffe and E. Leader, Sov. J. Nucl. Phys. **49** (1989) 136; M. Anselmino, A. Efremov and V. Leader, Phys. Rept. **261** (1995) 1; S. D. Bass, "The Drell-Heran-Gerasimov" sum rule in QCD", hep-ph/9703254
3. D. Drechsel et al., J. Phys. G: Nucl. Part. Phys. **18** (1992) 449; J. Soffer and O. Teryaev, Phys. Rev. Lett. **70** (1993) 3373
4. S. B. Gerasimov, Sov. J. Nucl. Phys., **2** (1966) 430; S. D. Drell and A. C. Hearn, Phys. Rev. Lett., **16** (1966) 908

5. Z. P. Li and Z. J. Li, Phys. Rev. D**50** (1994) 3119; R. Pantforder, H. Rollnik and W. Pfeil, "The Gerasimov-Drell-Heran sum rule and the infinite-momentum limit", hep-ph/9703668; S. Scopetta, A. Yu. Umnikov, C. Ciofi Degli Atti, and L. P. Kartari, "Nucleon and nuclear spin structure function", nucl-th/9709015
6. Z. P. Li, Phys. Rev. D**48** (1993) R3945
7. J. Ashamn et al., Phys. Lett. B**206** (1988) 364, Nucl. Phys. B**328** (1989) 1
8. V. Burkert and Z. J. Li, Phys. Rev. D**47** (1993) 47; V. Burkert and B. L. Ioffe, Phys. Lett. B**296** (1992) 223
9. Z. P. Li, Phys. Rev. D**47** (1993) 1954; Z. P. Li and Y. B. Dong, Phys. Rev. D**54** (1996) 4301
10. X. Ji, Phys. Lett. B**309** (1993) 187; X. Ji and P. Unrau, Phys. Lett. B**333** (1994) 228
11. K. Abe, et al., Phys. Rev. Lett. **78** (1997) 815
12. L.M. Stuart, et al., "Measurements of the $\Delta(1232)$ transition Form Factor and the Ratio σ_n/σ_p from Elastic-Proton and Electron-Deuteron Scattering", SLAC-PUB-7391
13. J. Ahrens, Mainz Proposal, 12/2-93, 1993; J. Ahrens et al., A2 Annual Report of 1996, Mainz
14. T. Iwata, "GDH sum rule with GeV photon", in "Quark Nucleon Physics with Multi-GeV Photon Facility at Spring-8", RCNP-P-134, (1995)
15. Z. E. Meziani, "Measurement of the neutron (^3He) spin structure function at low Q^2; a Connection between the Bjorken and the GDH sum rules", CEBAF Proposal No. 94-010
16. F. E. Close, In Introduction of Quarks and Partons, (Academic Press, London, 1979); B. L. Ioffe, V. A. Khoze, and L. N. Lipatov, "Hard processes", North-Holland, New York (1983)
17. D. Drechsel et al., Prog. Part. Nucl. Phys. **34** (1995) 181
18. M. MacCormick, et al., Phys. Rev. C**53** (1996) 41
19. N. Bianchi, et al., Phys. Lett. B**299** (1993) 219
20. N. Bianchi, et al., Phys. Lett. B**309** (1993) 5
21. N. Bianchi, et al., Phys. Rev. C**54** (1996) 1688; and private communication
22. W. Cassing et al., Phys. Rep. **188** (1990) 363; R. A. Arndt et al., Phys. Rev. C**42** (1990) 1853; D**43** (1991) 2131
23. M. Effenberger, A. Hombach, S. Teis, and U. Mosel, Nucl. Phys. A**613** (1997) 501; A**614** (1997) 353
24. R. L. Walker, Phys. Rev. **182** (1969) 1729
25. S. Teis et al., Z. Phys. A**356** (1997) 421
26. Particle Data Group, Phys. Rev. D50 (1994), 1173.
27. B. Krusche et al., Phys. Rev. Lett. **74** (1995) 3736
28. F. E. Close and Z. P. Li, Phys. Rev. D**42** (1992) 2194, 2207; S. Capstick, Phys. Rev. D**46** (1992) 1965, 2864
29. F. Foster and G. Hughes, Z. Phys. C**14** (1982) 123; M. Warn et al, Z. Phys. C**45** (1990) 627
30. Z. P. Li, Y. B. Dong, and W. H. Ma, J. Phys. G**23** (1997) 151
31. Z. P. Li, V. Burkert, and Z. J. Li, Phys. Rev. D**46** (1994) 70
32. S. J. Brodsky and J. Primack, Ann. Phys. (N. Y.) **52** (1969) 315
33. E143, K. Abe et al., Phys. Lett. B**364** (1995) 61
34. L. A. Kondratyuk, et al., Nucl. Phys. A**579** (1994) 453
35. L. N. Chang, Yigao Liang, and R. L. Workman, Phys. Lett. B**329** (1994) 514
36. P. Stoler, Phys. Rept. **226** (1993) 103
37. T. Sato, T. -S. H. Lee, Phys. Rev. C**54** (1996) 2660
38. R. A. Arndrt, R. L. Workman, Z. J. Li, and L. D. Roper, Phys. Rev. C**42** (1990) 1853; 1864